engineering proceedings

MDPI

Proceeding Paper

Modification of Aluminum 1050 and 2219 Alloys Using CuBr Nanosecond Laser for Hydrophobic and Hydrophilic Properties †

Antons Pacejs [1,*], Emil Yankov [2,*], Imants Adijans [1], Edmunds Teirumnieks [1] and Lyubomir Lazov [1]

[1] Faculty of Engineering, Rezekne Academy of Technologies, 4601 Rezekne, Latvia; imants.adijans@rta.lv (I.A.); edmunds.teirumnieks@rta.lv (E.T.); lyubomir.lazov@rta.lv (L.L.)
[2] Materials Science and Technology, University of Ruse "Angel Kanchev", 7017 Ruse, Bulgaria
* Correspondence: antons.pacejs@rta.lv (A.P.); eyankov@uni-ruse.bg (E.Y.)
† Presented at the 4th International Electronic Conference on Applied Sciences, 27 October–10 November 2023; Available online: https://asec2023.sciforum.net/.

Abstract: This study investigates the use of a CuBr vapor nanosecond laser with a 510 nm/578.2 nm wavelength for the surface treatment of 1050 aluminum and 2219 aluminum alloys. Laser-induced periodic surface structuring was used to optimize processing parameters to achieve hydrophobic and hydrophilic properties on the surface. The wetting properties were measured and the roughness results (R_a, R_z, R_q) evaluated. Prior to and after laser treatment, surface wetting and roughness changes were investigated. The wetting study showed that the maximum contact angle between a droplet of deionized water and the treated surface can be reached between more than 140 degrees and less than 10 degrees, which, respectively, is a superhydrophobic and superhydrophilic surface. Compared with the untreated surface, wetting increased by more than 2 times and decreased by more than 8 times. Overall, experiments show the dependence of wetting properties on laser input parameters such as scan speed and scan line distance with different delivered energy amounts. This study demonstrates the possibility of laser parameter optimizations which do not require auxiliary gases and additional processing of the resulting surfaces to obtain different wetting properties on the surface. The findings described in this article suggest that the CuBr laser surface treatment method is a promising method for industrial applications where surfaces with special wetting and roughness properties are required, for example, the laser marking of the serial number of parts used in wet environments such as aerospace, shipbuilding, and defense industries.

Keywords: hydrophobic; hydrophilic; aluminum; roughness; laser texturing; CuBr laser

check for updates

Citation: Pacejs, A.; Yankov, E.; Adijans, I.; Teirumnieks, E.; Lazov, L. Modification of Aluminum 1050 and 2219 Alloys Using CuBr Nanosecond Laser for Hydrophobic and Hydrophilic Properties. *Eng. Proc.* **2023**, *56*, 326. https://doi.org/10.3390/ASEC2023-16582

Academic Editor: Nunzio Cennamo

Published: 4 December 2023

Copyright: © 2023 by the authors. Licensee MDPI, Basel, Switzerland. This article is an open access article distributed under the terms and conditions of the Creative Commons Attribution (CC BY) license (https://creativecommons.org/licenses/by/4.0/).

1. Introduction

Photon–electron interaction is a crucial technique used in surface science, materials science, and condensed matter physics. This phenomenon enables the study of surface properties at an atomic level [1]. Consequently, the material undergoes modifications in surface morphology, chemical composition, and surface properties [2]. Nanosecond lasers find use in many industrial applications; therefore, picosecond and femtosecond lasers are useful in applications that require high precision and minimal damage to the surrounding material. All three types of lasers have their advantages and disadvantages and complement each other in various industrial applications [3]. Laser-based surface treatments can modify the surface structure of a material, leading to changes in its surface energy and wetting properties. Limited research has been conducted to examine the surface's long-term durability against organic contamination [4]. Currently, there is a limited amount of research on the utilization of CuBr vapor lasers for aluminum treatment. One of the studies in this area focuses on titanium ablation using a CuBr laser [5], while another study in 2021 achieved a record high average laser power of 140 W through the use of an atomically self-terminating CuBr vapor laser [6]. However, there is a lack of literature

on the use of CuBr vapor lasers for material treatment and investigating roughness and wetting properties, as this has not been explored in previous studies. The present study aimed to investigate the effects of Copper Bromide vapor nanosecond laser treatment on the surface morphology, roughness, and wetting properties of aluminum 1050 and aluminum 2219 alloys. In a recent report, A.O. Ijaola et al. [7] conducted a review on the surface wetting properties of different materials research published between the years 2003 and 2022. The report provides a comprehensive and critical analysis of superhydrophobic surfaces that have been laser textured on different substrate materials. In another review article, M.M. Quazi et al. [8] provided a summary of the surface treatment and modification of aluminum and its alloys using laser systems such as CO2, diode laser, Nd:YAG, Yb-Fiber, Ruby, and Excimer. The article also offers an overview of the various techniques employed in the laser surface treatment of aluminum and its alloys. D.V. Zaitseva et al. [9] reported on the behavior of water droplets on laser-modified surfaces of aluminum alloy (AMg6). The surfaces were modified using laser ablation with a 1064 nm Ytterbium nanosecond pulsed fiber laser. The article provides details on the experiment and the observed behavior of the water droplets on the laser-modified surfaces. M.V. Rukosuev et al. [10] conducted research on the use of femtosecond laser ablation as a potential method for producing hydrophobic micro- and nanostructures on austenitic stainless steel (AISI 316L) surfaces. The authors successfully generated hierarchical structures on the surface, which led to superhydrophobic properties. Additionally, laser ablation of the surfaces resulted in dual-scale hierarchical structures, further enhancing the hydrophobicity to a 167° contact angle (CA). The study demonstrates the potential of femtosecond laser ablation as a method for creating hydrophobic surfaces with micro- and nanostructures on AISI 316L. L. Ruiz de Lara et al. [11] conducted a study on the formation of laser-patterned ultrahydrophobic aluminum surfaces and evaluated their corrosion resistance using polarization curves and open circuit potential measurements. The article describes the process of creating these surfaces using laser patterning techniques and provides details on the testing methods used to assess their corrosion resistance. The study highlights the potential of laser patterning to create ultrahydrophobic surfaces with improved corrosion resistance properties. In another research study, Rafieazad Mehran et al. [12] showed that surface hydrophobicity does not necessarily improve the corrosion resistance of a sample. The article presents a critical evaluation of the relationship between surface hydrophobicity and corrosion resistance and highlights the need for further investigation to better understand this relationship. Zhenhui Chen et al. [13] used a picosecond laser to modify the surface of a pure aluminum sheet with a wavelength of 1064 nm, a repetition rate of 1000 kHz, and a scanning speed of 0.4 m/s. The laser treatment resulted in a superhydrophilic and light absorbent surface, which the authors suggest may be suitable for enhancing the efficiency of solar desalination. The study suggests that picosecond laser-treated aluminum surfaces have significant potential for sustainable desalination applications. As such, the utilization of a CuBr vapor laser to achieve similar results could be a promising area for further research. To conclude, limited research exists on the effects of dual-wavelength CuBr laser treatment on materials, but this treatment has shown potential for enhancing the wetting and roughness properties of aluminum alloys, making it useful in industries such as aerospace, automotive, and construction.

2. Materials and Methods

2.1. Laser

The surfaces of aluminum alloy sheets were irradiated with a Copper Bromide vapor laser system (Institute of Solid State Physics, Sofia, Bulgaria) operating at dual wavelengths of 510 nm and 578.2 nm. To conduct material treatment experiments, a range of processing parameters were employed. These parameters included a scanning speed varying from 2 mm/s to 300 mm/s, a scanning interval varying between 10 µm and 90 µm, and an average power ranging from 2 W to 10 W. Additionally, the impulse width and repetition rate was set at 30 ns and 20 kHz, respectively, with an impulse energy of 1.2 mJ, beam

quality $M^2 < 1.5$, and laser spot diameter of 40 µm. The principal scheme of laser treatment experiments can be observed in Figure 1.

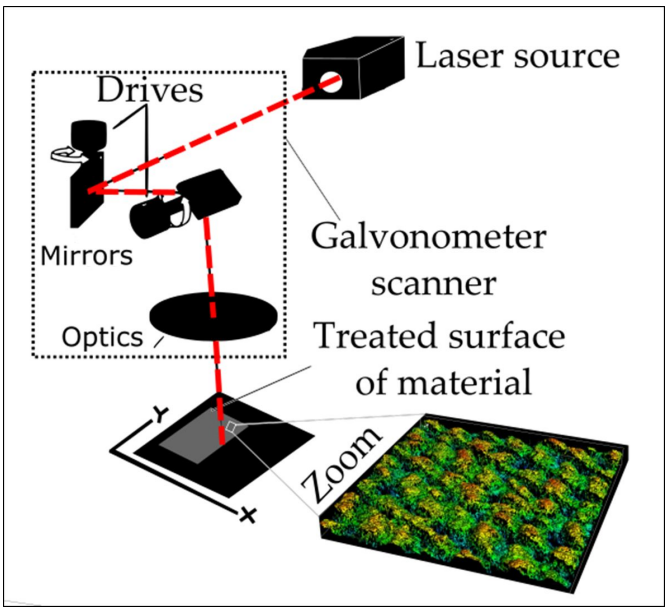


Figure 1. Schematic representation of laser treatment of samples.

The laser was focused onto the sample surface using an F-theta lens with a 30 µm spot size. More specific mechanical engineering details about the laser can be found in the research paper of the owner of this specific laser system [14]. To investigate the impact of laser processing parameters on material properties, a parameter matrix was developed in which two parameters were varied while others remained constant. Therefore, for a better understanding of the impact of laser processing parameters, mathematical equations can be employed to establish correlations between the processing parameters and the resulting material properties, e.g., the roughness and wetting.

Average energy density ($\bar{E}$) is a parameter in laser processing which determines the amount of average energy delivered per unit area to the material. It can be calculated by using Equation (1):

$$\overline{E} = \frac{(A \times P)}{(v \times \Delta x)}, \quad (1)$$

where A—coefficient of reflection for aluminum 0.7; P—average power of laser in W; v—scanning speed in mm/s; and Δx—distance between scanning lines in mm. The unit of average energy density is J/mm^2.

Pulse overlap (K_{ov}) is a parameter in laser processing which determines the pulse overlap in percent within a single laser scanning path. It can be calculated by using Equation (2):

$$K_{ov} = \left(1 - \frac{v}{f \times d}\right) \times 100 \quad (2)$$

where f—repetition rate frequency in Hz; v—scanning speed in mm/s; and d—diameter of the focal spot of the laser in mm. The unit of pulse overlap is percents.

2.2. Material

For this study, aluminum 2219 and 1050 alloy sheets with dimensions of 100 mm × 60 mm × 2 mm were used; see Table 1 with chemical compositions. The initial surface roughness, melting point, thermal conductivity, and initial surface contact angle (CA) of the aluminum alloys were evaluated.

Table 1. Chemical composition of aluminum alloy 2219 and aluminum alloy 1050.

Alloy	Chemical Composition (%)	Melting Point (°C)	Thermal Conductivity (W/m*K)	Initial Surface Roughness (µm)	Initial Surface (CA, °)
Aluminum 1050	Al: 99.6 ± 0.08, Si: 0.26 ± 0.025, Fe: 0.41 ± 0.01, Cu: 0.04 ± 0.03, Mn: 0.04 ± 0.02, Mg: 0.04 ± 0.02, Zn: 0.04 ± 0.01, Ti: 0.02 ± 0.01, Cr: 0.02 ± 0.01, Other: 0.02 ± 0.01	648 ± 3	221 ± 2	R_a = 0.156 ± 0.022 R_z = 3.97 ± 0.032 R_q = 0.201 ± 0.020	73 ± 1
Aluminum 2219	Al: 91.5 ± 0.51 Cu: 6.2 ± 0.60, Zn: 0.50 ± 0.20, Mn: 0.30 ± 0.10, Mg: 0.03 ± 0.07, Ti: 0.06 ± 0.04, Cr: 0.06 ± 0.04, Other: <0.10	542 ± 2	150 ± 2	R_a = 0.318 ± 0.020 R_z = 4.19 ± 0.029 R_q = 0.387 ± 0.018	68 ± 1

During the research, the materials—before the irradiance with the laser—were cleaned with isopropanol, dried, and kept in room temperature conditions for 24 h. After the laser treatment, the material samples were again cleaned with isopropanol in an ultrasound bath for 1 h and then dried and kept in room temperature conditions for 24 h. It should be noted that the material was not subjected to any mechanical treatment and that the surfaces observed in Figure 2 are made by the manufacturer.

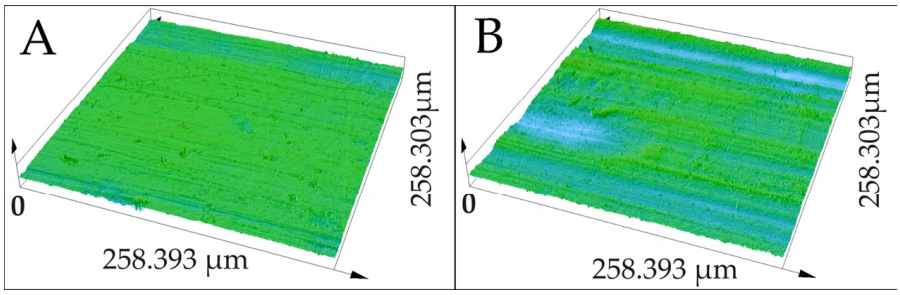


Figure 2. Material surface before laser treatment, where (**A**)—Al alloy 1050 and (**B**)—Al alloy 2219.

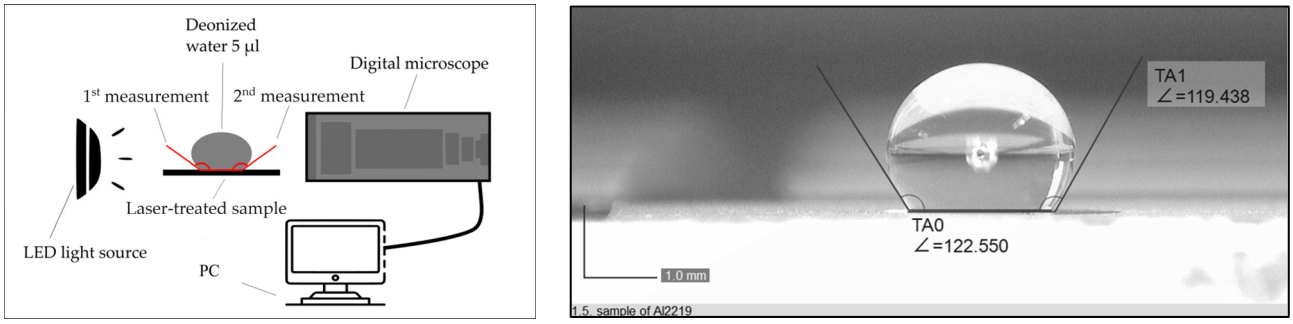
2.3. Wettability

The angle of the deionized water droplet was measured using a principal diagram, which is shown in Figure 3. A manual dosing micropipette was used for dosing the drop. The controlled dose of the drop was 50 µm, which was administered manually. On each marking, 5 consecutive measurements were carried out; the averaged value is presented in the results. It should be noted that the measurements were made in accordance with the ASTM D7334-08 (2022) standard.

2.4. Roughness

To measure surface roughness, an Olympus OLS 5000 laser scanning microscope with an ×50 lens which ensures ×1125 magnification and a scan area of 258 µm × 258 µm was selected to conduct measurements. It should be noted that the laser scanning microscope was utilized to scan the sample surface with a pitch of scanning of 0.4 µm, which corresponds to the "fine" measurement option in OLS software; then, the resulting data were analyzed using the built-in software to generate a 3D topography map, intensity profile,

and true color image of the sample in magnification. The roughness parameters R_a, R_q, and R_z were calculated from the 3D topography map automatically.



(**a**) (**b**)

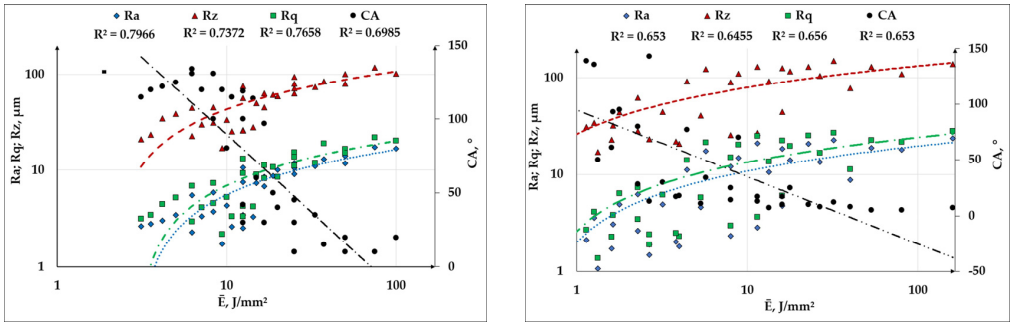
Figure 3. Wettability measurement scheme (**a**) of laser-treated samples and (**b**) view of CA measurement made in DinoLite software for single laser-treated sample.

3. Results and Discussion

In this section, the plotted data trends for wetting, roughness, and derived variable values that were obtained by the treatment of materials using a CuBr vapor laser with different processing parameters could be observed. Trend lines with a higher R-squared coefficient, indicating a stronger correlation were chosen for all plotted data. A difference in the laser-applied parameters for the two processed alloys appears because of the parameters' optimizations, which were made to obtain hydrophobic and hydrophilic properties on different aluminum alloy materials.

Two models can describe the correlation between surface roughness and hydrophobicity in the context of surface wettability. The Wenzel model predicts an increase in the apparent contact angle for hydrophobic surfaces and a decrease for hydrophilic surfaces as surface roughness increases. However, this model cannot describe the behavior of laser-textured surfaces that change the wettability of the surface from hydrophilic to hydrophobic. The Cassie–Baxter model assumes that droplets do not wet rough surfaces completely due to trapped air packs within the surface interstices, resulting in higher apparent contact angles on rough surfaces compared with smooth surfaces. The measured contact angles in this study are expected to fit the Cassie–Baxter model rather than the Wenzel model [12].

The average energy density ($\bar{E}$) delivered to the laser-treated samples and the roughness and contact angles are plotted in Figure 4. The plotted logarithmic trendlines have an R-squared value which indicates both a strong correlation and, in Figure 4b, a moderate-to-strong correlation between the variables.



(**a**) (**b**)

Figure 4. Plotted data of contact angle, roughness, and average energy density of CuBr laser delivered to (**a**) Al 2219 alloy and (**b**) Al 1050 alloy samples.

The initial roughness of the aluminum 2219 alloy was R_a = 0.318 µm, R_z = 4.19 µm, and R_q = 0.387 µm, and the contact angle was 68°. After laser processing with an average energy density of 6 J/mm^2 delivered on aluminum alloy 2219, the roughness increased to R_a = 5.52 µm, R_z = 44.51 µm, and R_q = 6.88 µm, and the contact angle reached a maximum of 134° (Figure 4a). By increasing the average energy density by 16.67 times up to 100 J/mm^2, the roughness R_a increased by 3.03 times, R_z increased by 2.30 times, and R_q increased by 2.95 times. This change also affected the contact angle, which decreased by 6.70 times up to 20°. The wettability relative to the initial material surface properties decreased by 1.97 times when an average energy density of 6 J/mm^2 was applied, resulting in a hydrophobic surface. Conversely, an increase in wettability by 3.40 times was achieved when an average energy density of 100 J/mm^2 was applied, resulting in a hydrophilic surface.

The initial surface roughness of the aluminum 1050 alloy was measured as R_a = 0.156 µm, R_z = 3.97 µm, and R_q = 0.201 µm, and the contact angle was 73°. After laser processing with an average energy density of 0.88 J/mm^2, the roughness increased to R_a = 2.04 µm, R_z = 24.094 µm, and R_q = 2.437 µm. As a result, the contact angle also increased to a maximum of 145° (Figure 4b). Further increasing the average energy density by 181.81 times to 160 J/mm^2 caused a significant increase in roughness, with R_a increasing by 11.55 times, R_z increasing by 5.74 times, and R_q increasing by 11.48 times. This change also affected the contact angle, which decreased by 20.74 times, reaching a value of only 7°. As a consequence of laser processing, the surface wettability was altered relative to the non-treated surface. Specifically, when an average energy density of 0.88 J/mm^2 was applied, the wettability decreased by 1.99 times, resulting in a hydrophobic surface. In contrast, by increasing the average energy density to 160 J/mm^2, the wettability also increased by 10.43 times, resulting in a hydrophilic surface.

Figure 5 shows that the 3D morphology obtained by laser scanning microscopy provides a reliable representation of the correlation between surface irregularities and wetting properties. In the sample with CA 130° (Figure 5D), the surface roughness creates micropockets in which air becomes caught, resulting in a high contact angle of the water droplet with a roughness of R_a = 5.91 µm, R_z = 45.03 µm and R_q = 7.39 µm. Moreover, a decrease in the CA between the water droplet and the sample is accompanied by an increase in the number of the micro-channels, which are interconnected and allow air to escape laterally during droplet–surface contact, thereby accelerating the wettability of the droplet to <10° where the trend for superhydrophilicity is observable (Figure 5A) with a roughness of R_a = 11.86 µm, R_z = 94.43 µm, and R_q = 15.29 µm.

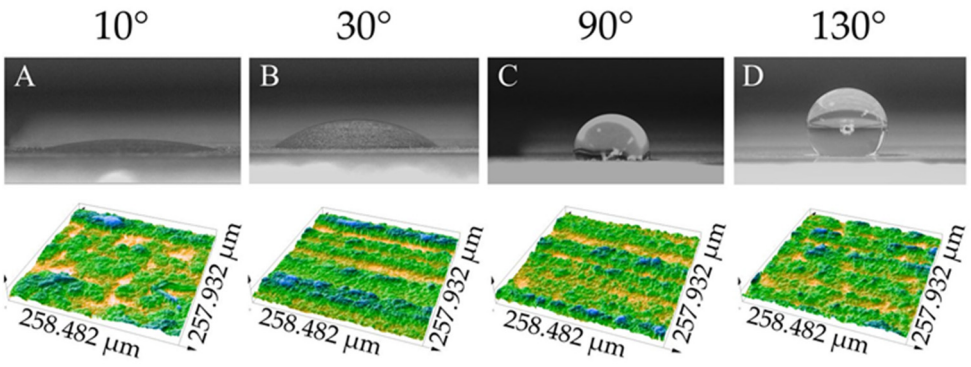


Figure 5. Droplets during the measurements of CA and laser-treated sample 3D surface morphologies of 2219 Al alloy.

Figure 6 data show that for the laser-treated specimen with CA 140° (Figure 6D), the roughness of the surface creates small pockets where air gets trapped, leading to a high contact angle of the water droplet. The roughness values for this surface are R_a 1.90, µm, R_z 23.047 µm, and R_q 2.41 µm. It should be noted that a decrease in the contact angle between the water droplet and the sample is accompanied by an increase in

the number of micro-channels that interconnect and allow air to escape laterally during droplet–surface contact, thus accelerating the wettability of the droplet. This results in a trend towards superhydrophilicity, as observable in Figure 5A. Therefore, the specimen shown in Figure 6A has roughness values of R_a 4.77 µm, R_z 44.35 µm, and R_q 6.07 µm.

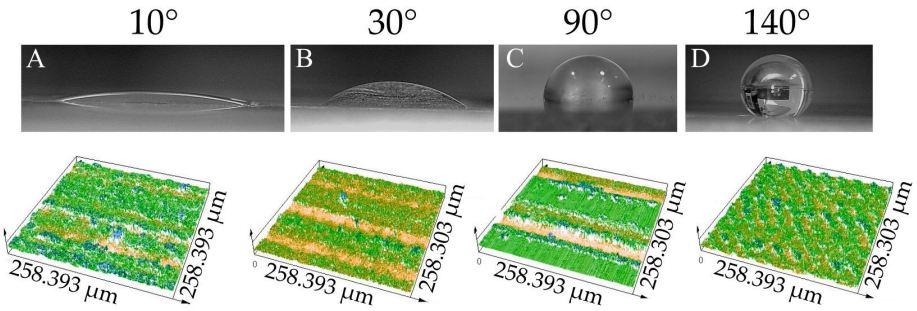
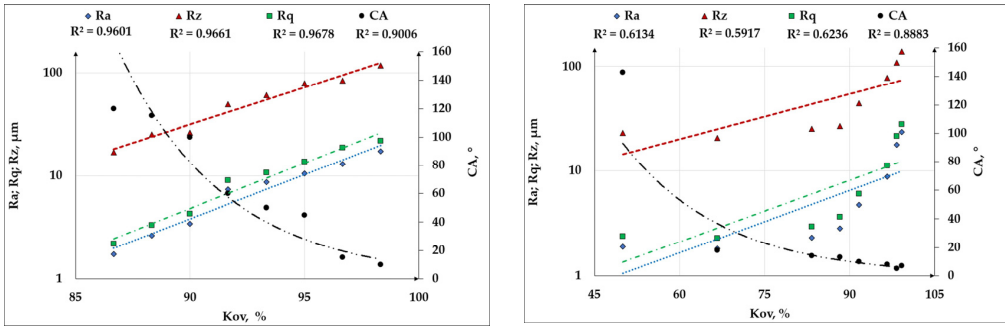


Figure 6. Droplets during the measurements of CA and laser-treated sample 3D surface morphologies of 1050 Al alloy.

In Figure 7, the pulse overlap (K_{ov}) is plotted together with roughness and CA. The trendlines for Figure 7a,b were exponential, with an R-squared value indicating a strong correlation for the Al 2219 alloy and a moderate correlation for the Al 1050 alloy.



(**a**) (**b**)

Figure 7. Plotted data of contact angle, roughness, and pulse density of CuBr laser processing at 8 W average power for the (**a**) Al 2219 and (**b**) Al 1050 alloy samples.

After laser processing with a pulse overlap of 98% on aluminum alloy 2219, the roughness increased to R_a = 11.86 µm, R_z = 94.43 µm, and R_q = 15.29 µm, and the contact angle reached CA 10° (Figure 7a).

By reducing the pulse overlap 1.05 times until reaching 93%, the roughness of R_a reduced by 2.14 times, R_z reduced by 2.12 times, and R_q reduced by 2.22 times. This change also affected the contact angle, which increased by 13.40 times up to CA 134° (Figure 7a). The wettability relative to initial material surface properties decreased 1.97 times when a pulse overlap of 93% was applied, resulting in a hydrophobic surface. Conversely, an increase in wettability by 6.8 times was achieved when a pulse overlap of 98% was applied, resulting in a hydrophilic surface with CA 10°. Adjusting the pulse overlap during laser processing of aluminum alloy 2219 can significantly alter surface roughness and wettability, with a 93% pulse overlap resulting in decreased roughness and hydrophobicity and a 98% pulse overlap resulting in increased wettability and hydrophilicity.

After subjecting aluminum alloy 1050 to laser processing with a pulse overlap of 99%, the surface roughness increased to R_a = 23.564 µm, R_z = 138.299 µm, and R_q = 27.965 µm, and the contact angle was CA 7°. When the pulse overlap was reduced by 1.22 times to 83%, the surface roughness reduced by 11.55 times for R_a, 5.74 times for R_z, and 11.48 times for R_q. This change also had an impact on the contact angle, which increased by 20.7 times to CA 145°, and the surface became hydrophobic, with a decrease in wettability by 1.99 times

relative to the initial material surface wetting. On the other hand, by applying a pulse overlap of 99%, the surface became hydrophilic, and the wettability increased by 10.42 times relatively to the non-treated sample. Modifying the pulse overlap during the laser processing of aluminum alloy 1050 can lead to significant changes in surface roughness and wettability, with a decrease in pulse overlap resulting in decreased roughness and increased hydrophobicity and an increase in pulse overlap resulting in increased wettability and hydrophilicity.

The changes that occur during laser processing depend on the material physical properties, chemical composition, and the surface properties. The same laser processing parameters utilized on two materials from different groups results in different properties occurring on the surface, especially where the main factor is related to the physical process of such technologies.

4. Conclusions

Within this research study, it has been determined that the laser processing of materials similar in chemical composition shows a difference in the change of roughness and wetting properties on the surface. Thus, the following conclusions could be made out of this study, i.e., the critical factors for change of roughness and wetting on the surface of treated materials are:

- Laser pulse overlap (K_{ov}), by increasing the overlap until reaching 98–99% roughness, increases gradually; this alters the transition to a hydrophilic surface CA 7°–10°. The main factor for the wetting change is the interconnected micro-channel formation on the surface via laser processing.
- Reducing the laser pulse overlap (K_{ov}) until reaching 83–93% reduces the roughness, thus decreasing the wettability; the surface obtains hydrophobic properties of 130°–145°. The main factor for the wetting change is the micro air pocket formation on the surface via laser processing.
- Increasing the average energy density ($\bar{E}$) delivered to the material by 100–160 J/mm^2 results in roughness increments, thus altering the transition to a hydrophilic surface CA 7°–10°.
- Decreasing the average energy density ($\bar{E}$) delivered to the material by 0.88–6 J/mm^2 results in roughness decrease, and the surface obtains hydrophobic properties of 130°–145°.

Author Contributions: Conceptualization, A.P., E.Y. and L.L.; methodology, A.P. and E.Y.; software, A.P. and E.Y.; validation, A.P., E.T., L.L. and E.Y.; formal analysis, A.P., E.Y. and I.A.; investigation, A.P., E.Y., I.A. and E.T.; resources E.T., E.Y. and L.L.; data curation, A.P. and E.Y.; writing—original draft preparation, A.P. and E.Y.; writing—review and editing, A.P., E.Y., L.L. and E.T.; visualization, A.P. and E.Y.; supervision, L.L. and E.T.; project administration, E.Y.; funding acquisition, E.Y., L.L. and E.T. All authors have read and agreed to the published version of the manuscript.

Funding: This research was funded by Ministry of Defense of the Republic of Latvia Nb.13.8/62 and Latvian Postdoctoral Research Support Program "Analysis of new industrial materials laser marking process parameters for high-tech applications" No. 1.1.1.2/VIAA/3/19/474.

Institutional Review Board Statement: Not applicable.

Informed Consent Statement: Not applicable.

Data Availability Statement: Data from our research can be found at https://conferences.rta.lv/index.php.

Acknowledgments: This work was developed within the framework of the "laser technology" research grant of the academic master's study program of Rēzekne Academy of Technologies of the Ministry of Defense of the Republic of Latvia Nb.13.8/62 and Latvian Postdoctoral Research Support Program "Analysis of new industrial materials laser marking process parameters for high-tech applications" No. 1.1.1.2/VIAA/3/19/474.

Conflicts of Interest: The authors declare no conflict of interest.

References

1. Jonasz, M.; Fournier, G. Chapter 1—Basic principles of the interaction of light with matter. In *Light Scattering by Particles in Water*; Jonasz, M., Fournier, G., Eds.; Academic Press: Cambridge, MA, USA, 2007; pp. 1–32, ISBN 9780123887511. [CrossRef]
2. Bloembergen, N. Laser-material interactions; fundamentals and applications. *AIP Conf. Proc.* **1993**, *288*, 3–10. [CrossRef]
3. Pou-Álvarez, P.; Riveiro, A.; Nóvoa, X.R.; Fernández-Arias, M.; del Val, J.; Comesaña, R.; Boutinguiza, M.; Lusquiños, F.; Pou, J. Nanosecond, picosecond and femtosecond laser surface treatment of magnesium alloy: Role of pulse length. *Surf. Coat. Technol.* **2021**, *427*, 127802. [CrossRef]
4. Zhang, L.; Zhao, N.; Xu, J. Fabrication and application of superhydrophilic surfaces: A review. *J. Adhes. Sci. Technol.* **2014**, *28*, 769–790. [CrossRef]
5. Balchev, I.; Minkovski, N.; Dimitrov, K.; Atanasov, A.; Stefanov, P. CuBr laser ablation of titanium surface. In Proceedings of the SPIE—The International Society for Optical Engineering, Sozopol, Bulgaria, 29 September–3 October 2014. [CrossRef]
6. Kostadinov, I.K.; Temelkov, K.A.; Astadjov, D.N.; Slaveeva, S.I.; Yankov, G.P.; Sabotinov, N.V. High-power copper bromide vapor laser. *Opt. Commun.* **2021**, *501*, 127363. [CrossRef]
7. Ijaola, A.O.; Bamidele, E.A.; Akisin, C.J.; Bello, I.T.; Oyatobo, A.T.; Abdulkareem, A.; Kayode Farayibi, P.; Asmatulu, E. Wettability Transition for Laser Textured Surfaces: A Comprehensive Review. *Surf. Interfaces* **2020**, *21*, 100802. [CrossRef]
8. Quazi, M.M.; Fazal, M.A.; Haseeb, A.S.M.A.; Yusof, F.; Masjuki, H.H. Laser-based Surface Modifications of Aluminum and its Alloys. *Crit. Rev. Solid State Mater. Sci.* **2016**, *41*, 106–131. [CrossRef]
9. Zaitsev, D.V.; Batishcheva, K.A.; Kuznetsov, G.V.; Orlova, E.G. Prediction of water droplet behavior on aluminum alloy surfaces modified by nanosecond laser pulses. *Surf. Coat. Technol.* **2020**, *399*, 126206. [CrossRef]
10. Rukosuyev, M.V.; Lee, J.; Cho, S.J.; Lim, G.; Jun, M.B. One-step fabrication of superhydrophobic hierarchical structures by femtosecond laser ablation. *Appl. Surf. Sci.* **2014**, *313*, 411–417. [CrossRef]
11. de Lara, L.R.; Jagdheesh, R.; Ocaña, J.L. Corrosion resistance of laser patterned ultrahydrophobic aluminium surface. *Mater. Lett.* **2016**, *184*, 100–103. [CrossRef]
12. Rafieazad, M.; Jaffer, J.; Cui, C.; Duan, X.; Nasiri, A. Nanosecond Laser Fabrication of Hydrophobic Stainless-Steel Surfaces: The Impact on Microstructure and Corrosion Resistance. *Materials* **2018**, *11*, 1577. [CrossRef] [PubMed]
13. Chen, Z.; Lin, Y.; Qian, Q.; Su, P.; Ding, Y.; Tuan, P.D.; Chen, L.; Feng, D. Picosecond laser treated aluminium surface for photothermal seawater desalination. *Desalination* **2022**, *528*, 115561. [CrossRef]
14. Atanasov, A.; Lengerov, A. Increasing the effeciency of laser marking of aluminum alloys by double writing of the symbols. Environment. Technologies. Resources. *Proc. Int. Sci. Pract. Conf.* **2021**, *3*, 20–24. [CrossRef]

Disclaimer/Publisher's Note: The statements, opinions and data contained in all publications are solely those of the individual author(s) and contributor(s) and not of MDPI and/or the editor(s). MDPI and/or the editor(s) disclaim responsibility for any injury to people or property resulting from any ideas, methods, instructions or products referred to in the content.